energies

MDPI

Article

Power Supply Reliability Analysis of Distribution Systems Considering Data Transmission Quality of Distribution Automation Terminals

Fengzhang Luo [1], Nan Ge [1,*] and Jing Xu [2]

[1] Key Laboratory of Smart Grid of Ministry of Education, Tianjin University, Tianjin 300072, China; luofengzhang@tju.edu.cn
[2] State Grid Tianjin Electric Power Company, Tianjin 300010, China; phoenix_xu@163.com
* Correspondence: genan2017@tju.edu.cn

Abstract: A distribution automation system is the integration of physical power distribution systems and information systems. Its information system guarantees the safe operation and reliable power supply of physical systems by monitoring, collecting and transmitting information. In the information system, the remote terminal unit of distribution automation is the hub of the information system, connecting it to the physical power system. Considering the unreliability of terminal information transmission in the information system, this paper aims to build a model to quantitatively evaluate the impact of unreliable transmission information on the power supply reliability of distribution systems. Firstly, the m-segment and n-connection unit model of distribution feeders is established, and then, the power supply reliability indices in the process of handling feeder terminal unit error are analyzed and calculated under the configuration modes of "three-remote" and "two-remote" of remote terminals. Then, considering the impact of a transmission error in the information system, the reliability index calibration model under the condition of unreliable information transmission is established. Finally, a case study is presented to illustrate how the proposed model is implemented.

Keywords: distribution automation system; power supply reliability; remote terminal unit; unreliable information transmission

Citation: Luo, F.; Ge, N.; Xu, J. Power Supply Reliability Analysis of Distribution Systems Considering Data Transmission Quality of Distribution Automation Terminals. *Energies* **2023**, *16*, 7826. https://doi.org/10.3390/en16237826

Academic Editor: Javier Contreras

Received: 8 November 2023
Revised: 27 November 2023
Accepted: 27 November 2023
Published: 28 November 2023

1. Introduction

A distribution automation (DA) system is the integration of modern electronic, optic, and wireless communication technology and network technology to remotely monitor, coordinate, and manage the physical components of a distribution system in a real-time information mode [1]. DA is an important guarantee for the stable operation and reliable power supply of power systems, and it has become an important part of smart grids and energy interconnection networks [2,3]. DA systems, in synergy with the control and protection systems, operate in the cyber–physical space of power distribution systems [4]. In certain large-scale architectures, DA systems are also interconnected with the automation, control and protection of power transmission and generation systems. DA systems can also be present in other utility industries, such as water and gas distribution systems [5,6].

A DA system is mainly composed of a communication network, DA main station and remote terminal units (RTUs). Where necessary, additional DA substations are installed. In addition, the DA main station also realizes data interactions with the production management system (PIM), geographic information system (GIS), outage management system (OMS), energy management system (EMS), customer information system (CIS) and other related systems through the information exchange bus. Figure 1 shows the system structure of an integrated DAS (distribution automation system). All the components, including the DA main station, DA substation, communication network and information exchange bus, as well as the sensors (distribution terminals), are referred to in this paper as the information parts of distribution systems.

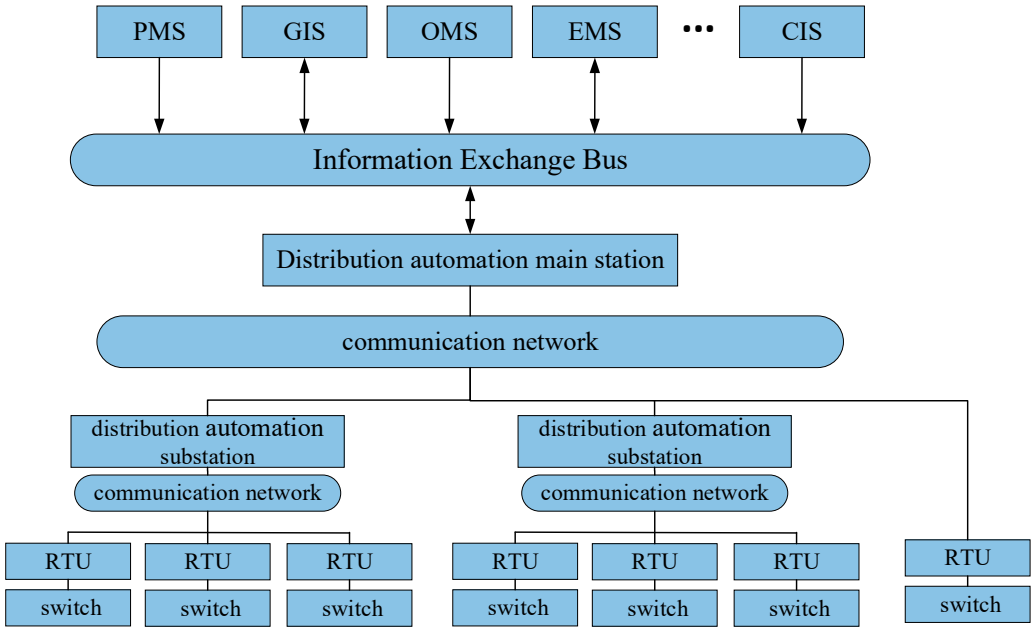

Figure 1. The system structure of an integrated DAS.

The RTU is in the sensor layer of DA and the hub of interactions between physical power systems and information systems, thus playing a key role in maintaining the reliability of distribution systems. Specifically, its functions include the following three aspects (Table 1) [7].

Table 1. Functions of RTU.

Function	Type of Collected or Operated Data	Application
remote measurement	operating parameters of distribution systems (U, I, P, f)	determining the location and type of failures
remote communication	real-time status of distribution equipment	delivery of real-time information
remote control	on–off state of switch	failure isolation and recovery

According to the functional configurations, RTUs can be divided into "three-remote (3R)" RTU and "two-remote (2R)" RTU. The "3R" RTU includes the functions of remote measurement, remote communication and remote control. It can realize automatic failure location detection and execute remote real-time control commands or complete the automatic isolation of local failures. The "2R" RTU includes the remote measurement function and the remote communication function. It can realize failure identification and failure information upload but cannot support remote control; thus, the failure has to be manually isolated. The realization of the three functions (including remote measurement, remote communication and remote control) of the RTUs is inseparable from the information transmission. Because RTUs are widely distributed but not fully covered, for the feeders equipped with RTUs, unreliable RTU information transmission may greatly affect the reliability index.

Regarding the physical network reliability of the distribution system, there are well-established assessment methods, primarily categorized into simulation and analytical methods. The core principle of these methods is the Failure Mode Effect Analysis (FMEA), involving an iterative search of the failure impact range and severity for components in all failure scenarios. The cumulative power outage levels at load points are assessed in each failure scenario, providing an evaluation of the distribution system's ability to provide a continuous power supply to electricity consumers.

The Monte Carlo simulation method [8–11] simulates device and system states, records failure events, and analyzes the impact of each failure event on system and customer out-

ages. While this method is conceptually simple, the accuracy of the results is inversely proportional to the computation time, with higher accuracy requiring longer computation times. Analytical methods for reliability assessment are primarily based on the network model of the distribution system. By enumerating all component failure events and analyzing the impact of each failure on the load, a set of system failure modes is formed, ultimately yielding reliability indicators for load nodes and the system as a whole. For instance, the Minimum Path Method [12,13] calculates reliability indicators for the system by considering only the components on the minimum path. Network equivalence methods [14] reduce the computational effort in reliability indicator calculations through rational boundary unit equivalence. Failure traversal methods [15] determine the failure type of the load based on the switch states of each node, enabling the calculation of reliability indicators. These methods effectively assess the physical network reliability of distribution systems, providing a reliability assessment framework for coordinated energy information distribution systems.

In addition to optimizing configurations using sectionalized switches and tie switches to enhance the reliability of the power distribution system [16], research on the reliability of information–physical power systems has also become a crucial focus in the industry. It can be observed that the distribution communication network and the distribution RTU are important components in the information system, and have significant impacts on the reliability of the power distribution system. Thus, the current research on the reliability of the DA system mainly focuses on two aspects: the distribution communication network and distribution RTU.

The research on the reliability of distribution communication networks focuses on various types of communication systems used in power systems, such as SCADA systems [17,18], wide-region closed-loop control systems [19], wide-region protection systems [20], and cyber–physical coupling of distribution networks [21], but there is a lack of further research on the impact of an information system error on physical power systems. The research on distribution RTU mainly focuses on the influence of the type and location of RTUs on the reliability of power systems, but does not take into account the impact of the terminal data communication error on the reliability of distribution systems.

At present, there are some studies about information transmission in DA, which mainly focus on the design of the distribution automation information security scheme [22], information security assessment [23], detection [24] and information communication [25,26]. Considering the massive integration of components in the power distribution system [27], the surge in heterogeneous data from multiple sources [28], and the diverse and ecological requirements of electricity business applications [29], a type of cloud–edge collaborative data transmission and computing technology based on RTUs has emerged [30]. However, there is a gap in the research regarding the impact of information system data transmission errors on the reliability of physical systems. There is still much basic work needing to be urgently carried out on how to consider the impact of the unreliable information transmission of the RTUs on the distribution system's supply reliability. This paper aims to address this gap by conducting relevant research on the influence of information system data transmission errors on the reliability of physical systems.

The information part has a non-negligible impact on the safe and reliable power supply of the managed physical system [4]. If the RTU fails or an information transmission cyber error happens due to uncontrollable factors, the DA main station will receive the wrong data and refuse to execute the command, thus affecting the reliability of the entire distribution system. Moreover, due to the communication congestion, communication delay, interruption and other errors [31], unbearable disturbance may also lead to untimely feedback to the physical power system [32,33], affecting the reliability of the distribution system.

In order to understand the impact of the unreliable information transmission on the distribution system reliability, this paper firstly builds the reliability index calculation model based on the failure location, isolation and recovery process. Then, the calibration model of the reliability indexes and the calibration strategy are proposed considering the impact

of the unreliable information transmission system. Finally, the impact of the unreliable information transmission on the reliability indices are quantified via the System Average Interruption Duration Index (SAIDI) and the Expected Energy Not Supplied (EENS). The effectiveness of the model and algorithm are verified using case studies.

2. Reliability Assessment Preliminary Model and Fundamental Principles

2.1. M-Segment and N-Connection Structure of Distribution System

For simplicity, the power supply reliability studied in this paper is mainly focused on the feeder remote terminal unit with the segment switch and the tie switch. The actual distribution network can be simplified as a series of feeder sections with the segment and tie switches [34]. A typical multi-sectioned and multi-linked diagram of a feeder trunk is shown in Figure 2.

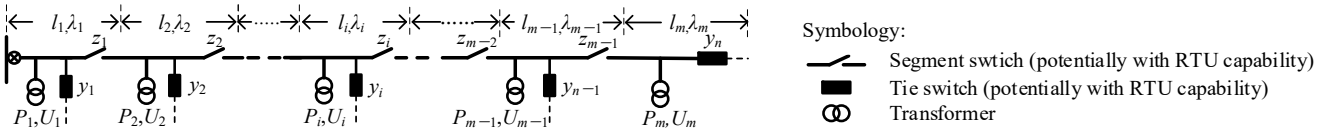

Figure 2. Typical feeder trunk diagram with m-segment and n-connection structure.

In Figure 2, the feeder contains $m-1$ segment switches and contains n tie switches (generally $m \geq n$). i is the label of the segmented region, which represents the ith section region. The section whose order is smaller than i (e.g., $i-1$) is its upstream segment. And the section whose order is greater than i (e.g., $i+1$) is its downstream segment. P_i represents the sum of the equivalent loads of the ith segmented region; U_i represents the total number of customers of the ith segmented region; l_i represents the equivalent line length of the ith segmented region; λ_i represents the failure rate of segment i. z_k represents whether the distribution automation terminal is configured at the position of the segment switch. $z_k = 1$ shows that the corresponding switch has a RTU and $z_k = 0$ shows that the switch does not have a RTU. Similarly, y_n represents the configuration state of the tie switch. This work assumes that all RTUs are powered by reliable PV solar power with batteries or an alternative power supply with a negligible failure rate. Also, it is assumed that all RTUs have a fail-safe functionality, internal batteries, self-diagnosing and self-healing capability after failure of the power supply for the RTUs.

2.2. Principle of Failure Mode Effect Analysis (FMEA)

The most fundamental principle in the reliability analysis of distribution systems is the Failure Mode Effect Analysis (FMEA) method, which was first applied to the field of power system reliability assessment by R. Billinton [35]. In this paper, SAIDI and EENS are taken as the measure to quantify the system's reliability, which are calculated with FMEA. In the FMEA model, one failure event can be divided into three main sub-processes: failure location, failure isolation, and failure recovery. Accordingly, the handling time of these three sub-processes can be expressed as follows:

$$T = T_1 + T_2 + T_3 \tag{1}$$

where T is the time required for the entire process of failure handling. To simplify the expression, the time required for the entire process of failure handling T can also be called the system interrupt duration (SID). T_1 is the failure detection time for the failure location phase; T_2 is the failure isolation time, that is, the time required for the failure to be effectively isolated; T_3 is the failure recovery time.

The corresponding electrical energy shortage in the system can also be expressed as follows:

$$E = E_1 + E_2 + E_3 \tag{2}$$

where E is the amount of electrical energy shortage in the system corresponding to the process of failure handling. To simplify the expression, the amount of power shortage E can be called the energy not supplied (ENS). E_1, E_2 and E_3, respectively, represent the ENS of the three sub-processes. The electrical energy amount is quantified in kWh.

3. Failure Mode Effect Analysis (FMEA) Model Considering DAS

Unreliable data communication, which occurs in the RTUs of the DAS, will significantly impact the efficiency and accuracy of the three sub-processes described in (1) and (2) above. Therefore, the SID and ENS will also deteriorate, which will further affect SAIDI and EEN. To study the impact of unreliable information communication on the failure handling process, in the following part, we firstly established a model of failure handling and reliability calculation under various configurations of distribution RTUs without the data communication system error. Then, the impact of the information transmission system error on the system reliability indices is further incorporated.

3.1. Distribution System Equipped with "3R" RTUs

For the distribution systems equipped with the "3R" RTUs, it is assumed that the failure occurs in the region of the feeder section i, and the SID and ENS indices are calculated in each time of the process of failure handling (T_1, T_2, and T_3).

3.1.1. Failure Location Time

Due to the remote measurement function, "3R" RTU can support timely failure location. The failure detection time t_{1i}, which is also the decision-making time of the DA software, can be approximated to zero. The corresponding SID in the failure location phase of the ith region is as follows:

$$T_{1i} = t_{1i} l_i \lambda_i U_i + t_{1i} l_i \lambda_i \sum_{\substack{j=1 \\ j \neq i}}^{m} U_j \approx 0 \tag{3}$$

where t_{1i} is the failure detection time for the ith region. The first part of (3) shows the SID in the ith region, while the second part represents the SID of other parts of the system caused by the failure of the ith region.

The corresponding ENS is calculated as follows:

$$E_{1i} = t_{1i} \cdot l_i \cdot \lambda_i \cdot P_i + t_{1i} \cdot l_i \cdot \lambda_i \cdot \sum_{\substack{i=1 \\ i \neq i}}^{m} P_j \approx 0 \tag{4}$$

where the first part of (4) shows the ENS within the ith region, and the second part indicates the ENS of other parts caused by the failure in the ith region.

3.1.2. Failure Isolation Time

Considering "3R" RTU's remote control function, it can support automatic failure isolation; thus, the failure load isolation time of each section t_{2i} can also be approximated to zero. Therefore, the SID corresponding to the failure isolation phase of the ith region failure is as follows:

$$T_{2i} = t_{2i} \cdot l_i \cdot \lambda_i \cdot U_i + t_{2i} \cdot l_i \cdot \lambda_i \cdot \sum_{\substack{i=1 \\ i \neq i}}^{m} U_i \approx 0 \tag{5}$$

where t_{2i} is the failure isolation time for the ith region. The first part of (5) shows the SID in the ith region, while the second part represents the SID of other part of the system caused by the failure of the ith region.

The corresponding ENS is as follows:

$$E_{2i} = t_{2i} \cdot l_i \cdot \lambda_i \cdot P_i + t_{2i} \cdot l_i \cdot \lambda_i \cdot \sum_{\substack{i=1 \\ i \neq i}}^{m} P_i \approx 0 \tag{6}$$

where the first part of (6) shows the ENS in the ith region, while the second part indicates the ENS of the rest of the system caused by the failure in the ith region.

3.1.3. Failure Recovery Time

For the feeder branch without tie switches, the first section i and its downstream loads are de-energized when the section i is faulty. But for the upstream loads of the ith section, considering the installation of the RTUs, the power supply to part of the upstream loads can be restored via the action of the segment switches and the SID is approximately zero.

Therefore, the SID corresponding to the failure recovery process of the ith region is as follows:

$$T_{3i} = t_{3i} \cdot l_i \cdot \lambda_i \cdot U_i + t_{3i} \cdot l_i \cdot \lambda_i \cdot \left[\sum_{j=1}^{i-1} U_j \cdot \prod_{k=j+1}^{i} z_k \right] + t_{3i} \cdot l_i \cdot \lambda_i \cdot \left[\sum_{j=i+1}^{m} U_j \right] \tag{7}$$

where t_{3i} is the failure recovery time for the ith region. The first part of (7) shows the SID of the ith load, while the second and third parts represent the SID of the upstream loads and the downstream loads of the ith segment, respectively.

The corresponding ENS is as follows:

$$E_{3i} = t_{3i} \cdot l_i \cdot \lambda_i \cdot P_i + t_{3i} \cdot l_i \cdot \lambda_i \cdot \left[\sum_{j=1}^{i-1} P_j \cdot \prod_{k=j+1}^{i} z_k \right] + t_{3i} \cdot l_i \cdot \lambda_i \cdot \left[\sum_{j=i+1}^{m} P_j \right] \tag{8}$$

The first part of (8) shows the ENS for the system of the ith load, while the second and third parts represent the ENS for the upstream loads and the downstream loads.

For the feeder branch with the tie switch, the downstream loads and upstream loads can both be restored. Therefore, the SID corresponding to the failure recovery process of the ith region failure is as follows:

$$T_{3i} = t_{3i} \cdot l_i \cdot \lambda_i \cdot U_i + t_{3i} \cdot l_i \cdot \lambda_i \cdot \left[\sum_{j=1}^{i-1} U_j \prod_{k=j+1}^{i} z_k \right] + t_{3i} \cdot l_i \cdot \lambda_i \cdot \left[\sum_{j=i+1}^{m} U_j \prod_{k=i+1}^{j} z_k \right] \tag{9}$$

The corresponding ENS is as follows:

$$E_{3i} = t_{3i} \cdot l_i \cdot \lambda_i \cdot P_i + t_{3i} \cdot l_i \cdot \lambda_i \cdot \left[\sum_{j=1}^{i-1} P_j \cdot \prod_{k=j+1}^{i} z_k \right] + t_{3i} \cdot l_i \cdot \lambda_i \cdot \left[\sum_{j=i+1}^{m} P_j \cdot \prod_{k=i+1}^{j} z_k \right] \tag{10}$$

3.2. Distribution System Equipped with "2R" RTUs

The sub-processes of the failure location and failure recovery for the system equipped with "2R" RTUs are the same as those of the system equipped with "3R" RTUs. The only difference is the failure isolation sub-process. Automatic circuit recloser with automatic-manual local command is not considered in this research.

As the "2R" RTU does not have the remote control function, the failure needs to be manually isolated. Therefore, the SID and the ENS corresponding to the failure isolation process are consistent with those of the (5) and (6), but the results are not zero considering that the failure load isolation time t_{2i} of each region in (5) and (6) cannot be neglected. The automatic circuit recloser with automatic–manual local command is not considered in this research.

3.3. Distribution System Equipped with Both "3R" and "2R" RTUs

For the system equipped with both "3R" and "2R" RTUs, the failure location process and failure recovery process are consistent with those of the system completely equipped with "3R" RTUs. Therefore, only the failure isolation stage of the failure handling process should be analyzed.

Consider the cooperation strategy of the "3R" and "2R" RTUs: Firstly, the "3R" RTUs are installed at both ends of the feeder trunk, that is, at the positions of line outlet and the tie switch. Secondly, no matter where the failure of the feeder occurs, it is always preferred to operate the two "3R" RTUs closest to the failure region to ensure that the loads in the regions before or after the corresponding "3R" RTUs can always be effectively isolated. Finally, if there are "2R" RTUs equipped in the failure region where two "3R" RTUs are equipped at both ends, it is necessary to manually isolate the load to ensure that the failure isolation region is the smallest.

It is assumed that there are $M-1$ segment switches of lines equipped with "3R" RTUs; therefore, the number of "3R" regions divided by all of the "3R" switches is M. Compared to the feeder region division shown in Figure 2, the number of segment switches of lines equipped with "3R" RTUs, denoted as $M-1$ in this case, will not be greater than the total number of segment switches denoted as $m-1$ in Figure 2. In order to analyze the system SID and ENS in the failure isolation process, use $\Omega_{i'}$ to represent the set of customer indices contained in the i'th "3R" region; $|\Omega_{i'}|$ is the total number of customers included in the region. The event group vector $W = (w_1, w_2, \ldots, w_{2i'-1}, w_{2i'}, \ldots, w_{2M-1}, w_{2M})$ includes a total of two M events. It contains two meanings: firstly, it indicates the "3R" region where the failure is located; secondly, it also indicates whether the "2R" RTU is equipped in the region. The specific explanations are as follows:

$w_{2i'-1}$: The failure occurs in the i'th "3R" region, and the region is equipped with a "2R" RTU;

$w_{2i'}$: The failure occurs the i'th "3R" region, but the "2R" RTU is not equipped in the region.

For example, $W = (0, 1, 1, 0, 0, 1)$ indicates that there are three "3R" regions divided by two segment switches. The first and third "3R" regions are not equipped with a "2R" RTU. The second "3R" region is equipped with a "2R" RTU.

Therefore, when the failure occurs, the SID time in the second stage of the failure handling is calculated as follows:

$$\begin{cases} T_{2i1} = t_{2i} \cdot l_i \cdot \lambda_i \cdot |\Omega_1| & event\ w_1 \\ T_{2i2} = t_{2i} \cdot l_i \cdot \lambda_i \cdot |\Omega_2| & event\ w_3 \\ \cdots\cdots & \cdots\cdots \\ T_{2ii'} = t_{2i} \cdot l_i \cdot \lambda_i \cdot |\Omega_{i'}| & event\ w_{2i'-1} \\ \cdots\cdots & \cdots\cdots \\ T_{2iM} = t_{2i} \cdot l_i \cdot \lambda_i \cdot |\Omega_M| & event\ w_{2M-1} \\ 0 & others \end{cases} \tag{11}$$

The corresponding ENS is calculated as follows:

$$\begin{cases} E_{2i1} = t_{2i} \cdot l_i \cdot \lambda_i \cdot \sum\limits_{j \in \Omega_1} P_j & event\ w_1 \\ E_{2i2} = t_{2i} \cdot l_i \cdot \lambda_i \cdot \sum\limits_{j \in \Omega_2} P_j & event\ w_3 \\ \ldots\ldots & \ldots\ldots \\ E_{2ii'} = t_{2i} \cdot l_i \cdot \lambda_i \cdot \sum\limits_{j \in \Omega_{i'}} P_j & event\ w_{2i'-1} \\ \ldots\ldots & \ldots\ldots \\ E_{2iM} = t_{2i} \cdot l_i \cdot \lambda_i \cdot \sum\limits_{j \in \Omega_M} P_j & event\ w_{2M-1} \\ 0 & others \end{cases} \tag{12}$$

3.4. General Formula for the ENS and SID

For the sake of simplicity and convenience, the SID and ENS calculation formulas of the above three configurations are shown in Tables 2 and 3.

Table 2. System SID calculation model based on FMEA.

Phase	Configured All with "3R" RTUs	Configured All with "2R" RTUs	Configured with Both "2R" and "3R" RTUs
Failure location T_1	0	0	0
Failure isolation T_2	0	$T_{2i} = K_{2i} \cdot \sum\limits_{i=1}^{m} U_i$ $T_2 = \sum\limits_{i=1}^{m} T_{2i}$	$\begin{cases} T_{2i1} = K_{2i} \cdot \lvert\Omega_1\rvert & event\ w_1 \\ \ldots\ldots & \ldots\ldots \\ T_{2iM} = K_{2i} \cdot \lvert\Omega_M\rvert & event\ w_{2M-1} \\ 0 & others \end{cases}$ $T_2 = \sum\limits_{j \in \Omega_1} T_{2i1} + \sum\limits_{j \in \Omega_2} T_{2i2} \cdots + \sum\limits_{j \in \Omega_M} T_{2iM}$
Failure recovery T_3	$T_{3i} = \begin{cases} V_T + K_{3i} \cdot \sum\limits_{j=i+1}^{m} U_j & y_n = 0 \\ V_T + K_{3i} \cdot \left[\sum\limits_{j=i+1}^{m} U_j \prod\limits_{k=i+1}^{j} z_k \right] & y_n = 1 \end{cases}$ $T_3 = \sum\limits_{i=1}^{m} T_{3i}$	$T_{3i} = \begin{cases} V_T + K_{3i} \cdot \sum\limits_{j=i+1}^{m} U_j & y_n = 0 \\ V_T + K_{3i} \cdot \left[\sum\limits_{j=i+1}^{m} U_j \prod\limits_{k=i+1}^{j} z_k \right] & y_n = 1 \end{cases}$ $T_3 = \sum\limits_{i=1}^{m} T_{3i}$	$T_{3i} = \begin{cases} V_T + K_{3i} \cdot \sum\limits_{j=i+1}^{m} U_j & y_n = 0 \\ V_T + K_{3i} \cdot \left[\sum\limits_{j=i+1}^{m} U_j \prod\limits_{k=i+1}^{j} z_k \right] & y_n = 1 \end{cases}$ $T_3 = \sum\limits_{i=1}^{m} T_{3i}$
Total		$T = T_1 + T_2 + T_3$	

Table 3. System ENS calculation model based on failure mode effect analysis.

Phase	Configured All with "3R" RTUs	Configured All with "2R" RTUs	Configured with Both "2R" and "3R" RTUs
Failure location T_1	0	0	0
Failure isolation T_2	0	$E_{2i} = K_{2i} \cdot \sum\limits_{i=1}^{m} P_i$ $E_2 = \sum\limits_{i=1}^{m} E_{2i}$	$\begin{cases} E_{2i1} = K_{2i} \cdot \sum\limits_{j \in \Omega_1} P_j\ event\ w_1 \\ \ldots\ldots \\ E_{2iM} = K_{2i} \cdot \sum\limits_{j \in \Omega_M} P_j\ event\ w_{2M-1} \\ 0\ others \end{cases}$ $E_2 = \sum\limits_{j \in \Omega_1} E_{2i1} + \sum\limits_{j \in \Omega_2} E_{2i2} \cdots + \sum\limits_{j \in \Omega_M} E_{2iM}$
Failure recovery T_3	$E_{3i} = \begin{cases} V_p + K_{3i} \cdot \sum\limits_{j=i+1}^{m} P_j & y_n = 0 \\ V_p + K_{3i} \cdot \left[\sum\limits_{j=i+1}^{m} P_j \cdot \prod\limits_{k=i+1}^{j} z_k \right] & y_n = 1 \end{cases}$ $E_3 = \sum\limits_{i=1}^{m} E_{3i}$	$E_{3i} = \begin{cases} V_p + K_{3i} \cdot \sum\limits_{j=i+1}^{m} P_j & y_n = 0 \\ V_p + K_{3i} \cdot \left[\sum\limits_{j=i+1}^{m} P_j \cdot \prod\limits_{k=i+1}^{j} z_k \right] & y_n = 1 \end{cases}$ $E_3 = \sum\limits_{i=1}^{m} E_{3i}$	$E_{3i} = \begin{cases} V_p + K_{3i} \cdot \sum\limits_{j=i+1}^{m} P_j & y_n = 0 \\ V_p + K_{3i} \cdot \left[\sum\limits_{j=i+1}^{m} P_j \cdot \prod\limits_{k=i+1}^{j} z_k \right] & y_n = 1 \end{cases}$ $E_3 = \sum\limits_{i=1}^{m} E_{3i}$
Total		$E = E_1 + E_2 + E_3$	

In Tables 2 and 3, $y_n = 1$ represents the feeder branch with the tie switch, and $y_n = 0$ represents the feeder branch without the tie switch. The parameters K_{2i}, K_{3i}, V_P and V_T are calculated as follows:

$$K_{2i} = t_{2i} \cdot l_i \cdot \lambda_i \tag{13}$$

$$K_{3i} = t_{3i} \cdot l_i \cdot \lambda_i \tag{14}$$

$$V_T = K_{3i} \cdot U_i + K_{3i} \cdot \left[\sum_{j=1}^{i-1} U_j \cdot \prod_{k=j+1}^{i} z_k \right] \tag{15}$$

$$V_P = K_{3i} \cdot P_i + K_{3i} \cdot \left[\sum_{j=1}^{i-1} P_j \cdot \prod_{k=j+1}^{i} z_k \right] \tag{16}$$

K_{2i} and K_{3i} are intermediate coefficients introduced for simplifying expressions, representing the failure isolation time and failure recovery time for an individual customer in the ith segment area, respectively. V_T represents a portion of the system SID caused by the failure recovery sub-process. Specifically, it considers the increase in the system SID resulting from the restoration of power to the load of the ith region and the upstream load served by segment switches equipped with distribution terminals. V_P represents a portion of the system ENS caused by the failure recovery sub-process. Specifically, it accounts for the increase in the system ENS during the power restoration process for the load of the ith region served by segment switches and the upstream load during the aforementioned transfer process.

4. Quantitative Assessment Model Considering Unreliable Information Transmission

Under the condition of unreliable information transmission system, the FMEA mode considering DA in Section 3 needs to be revised. The idea is as follows:

Firstly, based on concept of reliability state analysis, the state transition diagram of feeder during the process from failure occurrence to repair is constructed. Secondly, the error of the information transmission system is classified according to the characteristics of "3R", which contains remote measurement, remote communication and remote control functions. And then, the quantitative analysis model of the feeder failure is established considering unreliable information transmission by analyzing its influence on each stage of the failure handling process. Finally, the expected value analysis method is used to calculate the reliability index of the feeder. Considering the unreliable information transmission, the analysis of the state transition process after the feeder failure is shown in Figure 3.

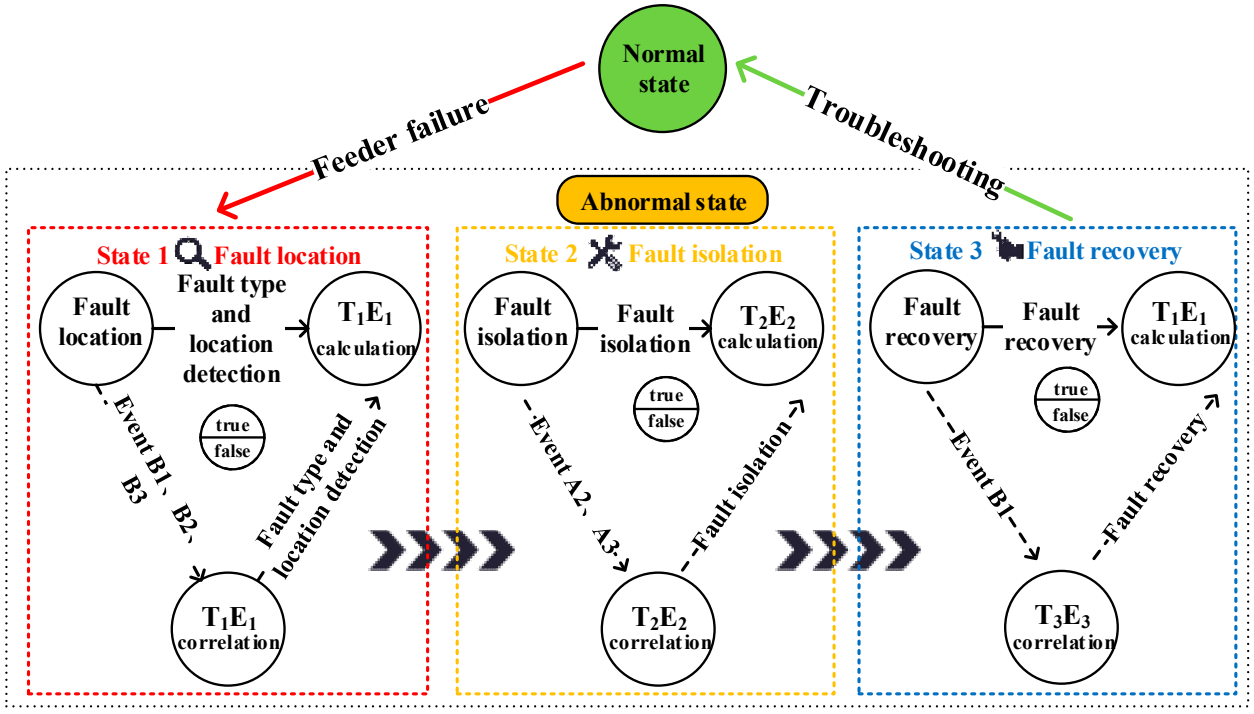

Figure 3. Feeder state transition models considering data communication errors of information system.

4.1. The Revised Model Equipped with "3R" RTUs

According to the coupling feature of the "3R" functions, the consequences of information transmission error (assuming that the probability of error occurrence is p) can be divided into the following three types of independent events (Table 4).

Table 4. Three types of independent events.

Event	Remote Communication and Remote Control	Remote Measurement
A	wrong	correct
B	correct	wrong
C	wrong	wrong

The analysis of the transmission error of the distribution RTU is as follows.

4.1.1. The Remote Communication and Remote Control Information Are Wrong, While the Remote Measurement Information Is Correct

Event A (assuming its probability of occurrence is p_1) can be divided into the following three types of independent sub-events:

a. Event A_1: The remote control information is correct, but the remote communication information is wrong. The probability of occurrence is set as p_{11}. In this condition, after the failure occurs, because the remote control can act correctly, the failure can be successfully isolated. However, the information that is reflected by the remote communication is still the information before the failure isolation, that is, the remote information reflects that the failure is not effectively isolated. Since the substation detects that the feeder is not faulty through the failure indicator, the remote communication function needs to be checked and the information needs to be corrected. Then, the failure recovery time should be corrected as follows (17):

$$t_{A_1} = t_3 + t_3^{11} \tag{17}$$

where t_3 represents the time for failure recovery when the remote communication information is accurate, and t_3^{11} represents the time for checking the remote communication functionality and correcting information. In this scenario, failure detection and the failure isolation time are considered unaffected.

b. Event A_2: The remote control information is wrong, but the remote communication is correct. The probability of occurrence is set as p_{12}. After the failure occurs, because the remote control information is incorrect, the failure is not effectively isolated. Therefore, the failure correctly reflected by the remote information is not isolated and the remote control function needs to be checked and the information needs to be corrected, and then the failure will be controlled. It is assumed that the RTU operates in a centralized monitoring mode, with maintenance personnel remotely monitoring the RTU from a control station and the RTU locking the manual isolation of the failure carried out by the local maintenance personnel. Since the failure is not effectively isolated, the ENS is expressed as follows:

$$E_{2i}^{12} = t_2'' \cdot L_i \cdot f_i \cdot \sum_{j=1}^{m} p_j + ENS_{2i} \tag{18}$$

where $t_2{}'' = t_2{}^{12}$ is the time required to check and correct the remote control signal and to re-isolate the failure. In this scenario, the failure detection time and failure recovery time are considered not affected. In practical scenarios, it is also conceivable to manually switch the RTU from remote control mode to local control mode, and the time required for this switch is included in the parameter $t_2{}''$.

c. Event A_3: The remote control and the remote communication information are both incorrect. The probability of occurrence is set as p_{13}. In this scenario, after the failure occurs, the failure is not effectively isolated due to the wrong remote control information, while the failure is reflected as being effectively isolated due to the incorrect remote communication. However, because the sub-station can detect that the feeder is faulty through the failure indicator, the remote control function and the remote communication function need to be checked, the remote control and remote communication signals need to be corrected, and finally, the failure re-isolation is carried out. As the failure is not effectively isolated, the system ENS of the failure isolation stage can be calculated as in (18). At this time, ${t_2}''$ in (18) needs to be replaced by ${t_2}^{13}$, and ${t_2}^{13}$ indicates the time required to check the function and to correct the information of remote control and remote communication. In this scenario, the failure detection time and failure recovery time are unaffected.

4.1.2. The Remote Communication and Control Information Are Correct but the Remote Measurement Information Is Wrong

According to the information collected via the remote measurement from DAS, the function of determining the failure location and failure type can be achieved. Accordingly, Event B (its probability is set as p_2) can be divided into the following three types of independent sub-events:

a. Event B_1: The remote measurement information error affects the determination of the failure location. The probability of occurrence is set as p_{21}. In this condition, after the failure occurs, the distribution RTU collects the information to determine the location of the failure according to the wrong information, affecting the effective isolation and recovery of the failure. At this point, it is necessary to check the remote measurement function and correct the information firstly, and then to find the correct failure location manually. Thus, the time of the failure location phase is corrected as follows (19):

$$t_{B_1} = t_1 + t_1^{21} \tag{19}$$

In this scenario, the failure isolation time and the failure recovery time are considered unaffected.

b. Event B_2: The remote measurement information error affects the determination of the failure type. The probability of occurrence is set as p_{22}. In this condition, after the failure occurs, the distribution RTU collects the information to determine the type of failure, but the wrong transmission information affects the effective failure isolation and recovery. At this point, it is needed to correct the remote measurement information and re-judge the type of failure in order to correctly isolate the failure.

The time to correct the remote measurement information and re-judge the failure type is ${t_1}^{22}$. The time of the failure location phase is as follows:

$$t_{B_2} = t_1 + t_1^{22} \tag{20}$$

In this scenario, the failure isolation time and the failure recovery time are considered unaffected.

c. Event B_3: The remote measurement information error affects both the detection of the failure location and the determination of the failure type. Setting the probability of occurrence as p_{23}, the time of the failure location phase is as follows:

$$t_{B_3} = t_1 + t_1^{21} + t_1^{22} \tag{21}$$

In this condition, the failure isolation time and the failure recovery time are considered unaffected.

4.1.3. Remote Control, Remote Communication and Remote Measurement Information Are Wrong

Since events A_1 to A_3 and events B_1 to B_3 belong to independent events, Event C (assuming the probability of occurrence p_3) can be obtained by combining events A_1 to A_3 and events B_1 to B_3.

The information system data transmission error of the event can be found in Figure 4.

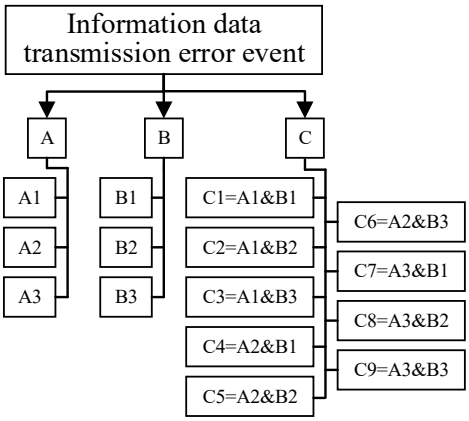

Figure 4. The relationship diagram of information transmission error events.

Assuming that the accuracy rate of remote control information is p_c, and the accuracy rate of remote communication, which can also be called remote signaling, is p_s, the accuracy rate of remote measurement information is p_m, which can be expressed as follows:

$$(1 - p_m) = p_{m1} + p_{m2} + p_{m3} \tag{22}$$

where p_{m1} represents the probability that the remote measurement information error incorrectly affects the failure location but does not affect the occurrence of the event with the determined failure type; p_{m2} represents the probability that the remote measurement information error incorrectly affects the type of failure but does not affect the failure event with the determined location; and p_{m3} represents the probability that the remote measurement information error affects the failure with the determined type and location.

Considering only the influence of the unreliable information transmission system, the probability and time correlation expressions of each corresponding event are shown in Table 5.

Table 5. Data transmission error calibration of information system equipped with three-remote RTUs.

Probability of the Transmission Error Events			Duration Calibration
$p = 1 - p_m \cdot p_c \cdot p_s$	$p_1 = (1 - p_c \cdot p_s) p_m$	$p_{11} = p_c \cdot (1 - p_s) \cdot p_m$	$t_{A1} = t_3 + t_3{}^{11}$
		$p_{12} = (1 - p_c) \cdot p_s \cdot p_m$	$t_{A2} = t_2 + t_2{}^{12}$
		$p_{13} = (1 - p_c)\,(1 - p_s) \cdot p_m$	$t_{A3} = t_2 + t_2{}^{13}$
	$p_2 = (1 - p_m) \cdot p_c \cdot p_s$	$p_{21} = p_c \cdot p_s \cdot p_{m1}$	$t_{B1} = t_1 + t_1{}^{21}$
		$p_{22} = p_c \cdot p_s \cdot p_{m2}$	$t_{B2} = t_1 + t_1{}^{22}$
		$p_{23} = p_c \cdot p_s \cdot p_{m3}$	$t_{B3} = t_1 + t_1{}^{21} + t_1{}^{22}$
	$p_3 = (1 - p_c \cdot p_s) \cdot (1 - p_m)$	$p_{31} = p_c \cdot (1 - p_s) \cdot p_{m1}$	$t_{C1} = t_{A1} + t_{B1}$
		$p_{32} = p_c \cdot (1 - p_s) \cdot p_{m2}$	$t_{C2} = t_{A1} + t_{B2}$
		$p_{33} = p_c \cdot (1 - p_s) \cdot p_{m3}$	$t_{C3} = t_{A1} + t_{B3}$
		$p_{34} = (1 - p_c) \cdot p_s \cdot p_{m1}$	$t_{C4} = t_{A2} + t_{B1}$
		$p_{35} = (1 - p_c) \cdot p_s \cdot p_{m2}$	$t_{C5} = t_{A2} + t_{B2}$
		$p_{36} = (1 - p_c) \cdot p_s \cdot p_{m3}$	$t_{C6} = t_{A2} + t_{B3}$
		$p_{37} = (1 - p_c)\,(1 - p_s) \cdot p_{m1}$	$t_{C7} = t_{A3} + t_{B1}$
		$p_{38} = (1 - p_c)\,(1 - p_s) \cdot p_{m2}$	$t_{C8} = t_{A3} + t_{B2}$
		$p_{39} = (1 - p_c)\,(1 - p_s) \cdot p_{m3}$	$t_{C9} = t_{A3} + t_{B3}$

Expressions (23)~(26) are used to modify the time of each stage by using the expected value analysis method.

a. Time calibration of the failure location phase:

$$\begin{aligned} t_1' = \; & t_1 \cdot p_1 + \left(t_1 + t_1^{21}\right) \cdot p_{21} + \left(t_1 + t_1^{22}\right) \cdot p_{22} \\ & + \left(t_1 + t_1^{21} + t_1^{22}\right) \cdot p_{23} + \left(t_1 + t_1^{21}\right) \cdot p_{31} + \left(t_1 + t_1^{22}\right) \cdot p_{32} \\ & + \left(t_1 + t_1^{21} + t_1^{22}\right) \cdot p_{33} + \left(t_1 + t_1^{21}\right) \cdot p_{34} + \left(t_1 + t_1^{22}\right) \cdot p_{35} \\ & + \left(t_1 + t_1^{21} + t_1^{22}\right) \cdot p_{36} + \left(t_1 + t_1^{21}\right) \cdot p_{37} + \left(t_1 + t_1^{22}\right) \cdot p_{38} \\ & + \left(t_1 + t_1^{21} + t_1^{22}\right) \cdot p_{39} + (1 - p) \cdot t_1 \end{aligned} \tag{23}$$

After simplification:

$$t_1' = t_1 + (p_{m1} + p_{m3}) \cdot t_1^{21} + (p_{m2} + p_{m3}) \cdot t_1^{22} \tag{24}$$

where the first part of (24) shows the failure detection time under normal circumstances. The second part of (24) represents the failure detection time under the condition that the remote measurement error affects the event with the determined location and the event with the determined type and location. The third part of (24) represents the failure detection time under the condition that the remote measurement error affects the event with the determined failure type and the event with the determined type and location.

b. Time calibration of the failure isolation phase:

$$t_2'' = t_2 + (1 - p_c) \cdot p_s \cdot t_2^{12} + (1 - p_c) \cdot (1 - p_s) \cdot t_2^{13} \tag{25}$$

where the first part of (25) represents the failure isolation time under the normal circumstances. The second part of (25) represents the impact of the incorrect remote control information but correct remote communication information on the failure isolation time. The third part of (25) represents the impact of the incorrect remote control information and remote communication information on the failure isolation time.

c. Time calibration of the failure recovery phase:

$$t_3' = t_3 + p_c \cdot (1 - p_s) \cdot t_3^{11} \tag{26}$$

where the first part of (26) represents the failure recovery time under normal circumstances. The second part of (26) represents the impact of correct remote control information but incorrect remote communication information on the failure recovery time.

Substituting (24) to (26) into the corresponding formulas, the corrected SAIDI and the EENS can be calculated.

4.2. The Revised Model Equipped without "3R" RTUs

Without the "3R" RTUs, all the "2R" RTUs are configured. Considering the particularity of the remote communication function, the event that the information of RTU is transmitted incorrectly, the probability of its occurrence and the time calibration of its sub-event are all shown in Table 6.

Table 6. Data transmission error calibration of information system not equipped with "3R" RTUs.

Probability of the Data Transmission Error Events			Duration Calibration
$p = 1 - p_m$	$p_B = 1 - p_m$	$p_{21} = p_{m1}$ $p_{22} = p_{m2}$ $p_{23} = p_{m3}$	$t_{B1} = t_1 + t_1{}^{21}$ $t_{B2} = t_3 + t_1{}^{22}$ $t_{B3} = t_{B1} + t_{B2}$

Since all the RTUs are "2R" RTUs, the system does not have the remote control function. Therefore, the time calibration of all the "2R" RTUs is only considered in the failure location

phase. The time is corrected by using the expected value method, and the time for the calibration of the "2R" RTUs is shown in (27) (normally, $t_1 = 0$):

$$t_1' = t_1 + (p_{m1} + p_{m3}) \cdot t_1^{11} + (p_{m2} + p_{m3}) \cdot t_1^{12} \quad (27)$$

5. Case Analysis

5.1. Introduction of the Case

The impact of information transmission errors on the reliability of distribution systems lacks a benchmark for comparison at present. Therefore, this paper is based on the modification of the IEEE 33-node system to conduct a case study for analysis (shown in Figure 5). The system is divided into six sub-regional zones, denoted by z_1, z_2, z_3, z_4, z_5 and z_6, respectively, by the feeder outlet switch, segment switches at branch 1–2, 2–3, 4–5, 8–9, 14–15, and the tie switches on nodes 21, 6, 14, 17, 32 and 24, as shown in Figure 5. The "2R" RTUs are configured between the branch 1–2 and branch 14–15, and the "3R" RTU is arranged at branch 8–9 in Figure 5.

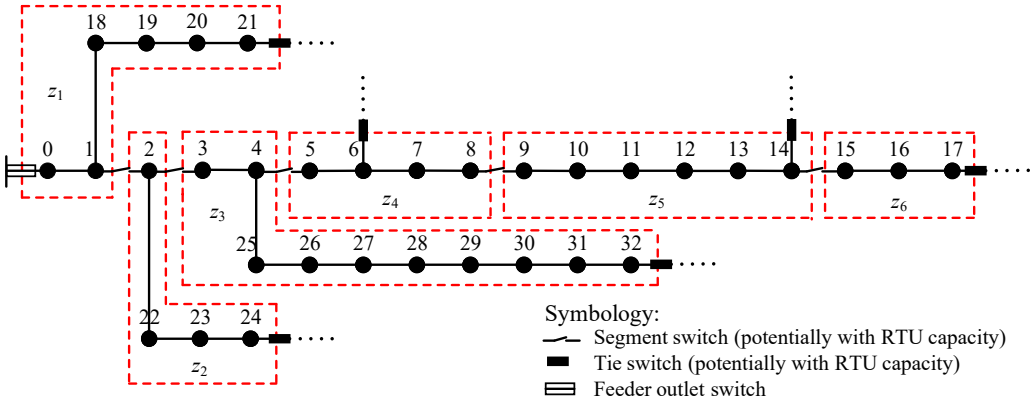

Figure 5. IEEE 33-node distribution system, "33" represents the presence of 33 load points (load point 0 to 32) in this system.

The zone loads of P_1, P_2 …, P_6 are 100 kW, 400 kW, 400 kW, 500 kW, 2500 kW and 400 kW, respectively. The number of customers in each segment region is 10, and the length of each zone's branches is 1.275 km, 0.26 km, 0.108 km, 0.17 km, 0.09 km and 0.22 km, respectively; the feeder failure rate is 0.23 times/km per year; and the failure handling time of the three sub-treatment phases t_1, t_2, t_3 is 1 h, 0.5 h and 4 h, respectively.

5.2. Verification of Accuracy

From a methodological perspective, the existing reliability assessment models for distribution systems provide a validation framework for this study. Therefore, taking the scenario of a fully reliable automation system as an example, the correctness of the proposed method is validated using the fault incidence matrix method [34]. The results are presented in Table 7.

Table 7. Verification of accuracy by taking the scenario of a fully reliable automation system as an example.

	Fault Incidence Matrix Method	**Proposed Method**
EENS (kW·h)	1443.99	1443.99
SAIDI (h)	38.4836	38.4836
ASAI (%)	99.56	99.56

After the comparison, the reliability indexes calculated using the method proposed in this paper are consistent with the results calculated via the fault incidence matrix

method [34]. In fact, the method proposed in this paper can be calculated by using the traditional failure mode and effect analysis method; thus, the accuracy of the algorithm proposed in this paper can be guaranteed.

5.3. Analysis of the Impact of Unreliable Information Transmission on the Reliability of Distribution System

By using the reliability evaluation method for the power distribution system with DAS, it would be easy to analyze the impact of unreliable information transmission on the reliability of the distribution system.

Three scenarios are considered.

Scenario 1: The automation system is 100% reliable.

Scenario 2: The accuracy rate of remote measurement and remote control is 100%, and the remote communication accuracy rate change is between 0 and 100%.

Scenario 3: The remote communication and remote measurement accuracy rate is 100%, and the remote control accuracy rate change is between 0 and 100%.

In addition, ${t_2}^{11} = 0.2$ h, ${t_2}^{12} = 0.4$ h, ${t_2}^{13} = 0.6$ h, ${t_1}^{21} = 0.15$ h, ${t_1}^{22} = 0.15$ h. Assuming that the error of the three scenarios corresponding to the probability of p_{m1}, p_{m2}, p_{m3} is the same, then $p_{m1} = p_{m2} = p_{m3} = (1 - p_m)/3$.

For the three scenarios mentioned above, Tables 8–10 show sensitivity analysis conducted by quantitatively analyzing the variations in reliability metrics under different levels of accuracy. Figure 6 shows the reliability indexes of the three scenes.

Table 8. Influence of remote communication accuracy rate changes on system annual energy not supplied and outage time.

Accuracy Change Rate of Remote Communication (%)	Change in EENS (kW·h)	Change Rate of EENS (%)	Change in SAIDI (h)	Change Rate of SAIDI (%)
100–95	1443.99–1446.61	0.1816	38.4836–38.5572	0.1913
95–90	1446.61–1449.23	0.1813	38.5572–38.6308	0.1909
90–85	1449.23–1451.85	0.1809	38.6308–38.7043	0.1903
85–80	1451.85–1454.47	0.1806	38.7043–38.7791	0.1933
80–75	1454.47–1457.1	0.1803	38.7791–38.8515	0.1867

Table 9. Influence of remote measurement accuracy rate changes on system annual energy not supplied and outage time.

Accuracy Change Rate of Remote Measurement (%)	Change in EENS (kW·h)	Change Rate of EENS (%)	Change in SAIDI (h)	Change Rate of SAIDI (%)
100–95	1443.99–1464.98	1.4542	38.4836–38.7766	0.7614
95–90	1464.98–1485.98	1.4332	38.7766–39.0695	0.7554
90–85	1485.98–1506.98	1.4129	39.0695–39.3625	0.7499
85–80	1506.98–1527.97	1.3933	39.3625–39.6555	0.7444
80–75	1527.97–1548.97	1.3742	39.6555–39.9485	0.7389

Table 10. Influence of remote control accuracy rate changes on system annual energy not supplied and outage time.

Accuracy Change Rate of Remote Control (%)	Change in EENS (kW·h)	Change Rate of EENS (%)	Change in SAIDI (h)	Change Rate of SAIDI (%)
100–95	1443.99–1485.98	2.9082	38.4836–39.0695	1.5225
95–90	1485.98–1527.97	2.8259	39.0695–39.6555	1.4999
90–85	1527.97–1569.97	2.7484	39.6555–40.2414	1.4775
85–80	1569.97–1611.96	2.6747	40.2414–40.8274	1.4562
80–75	1611.96–1653.95	2.6052	40.8274–41.4133	1.4351

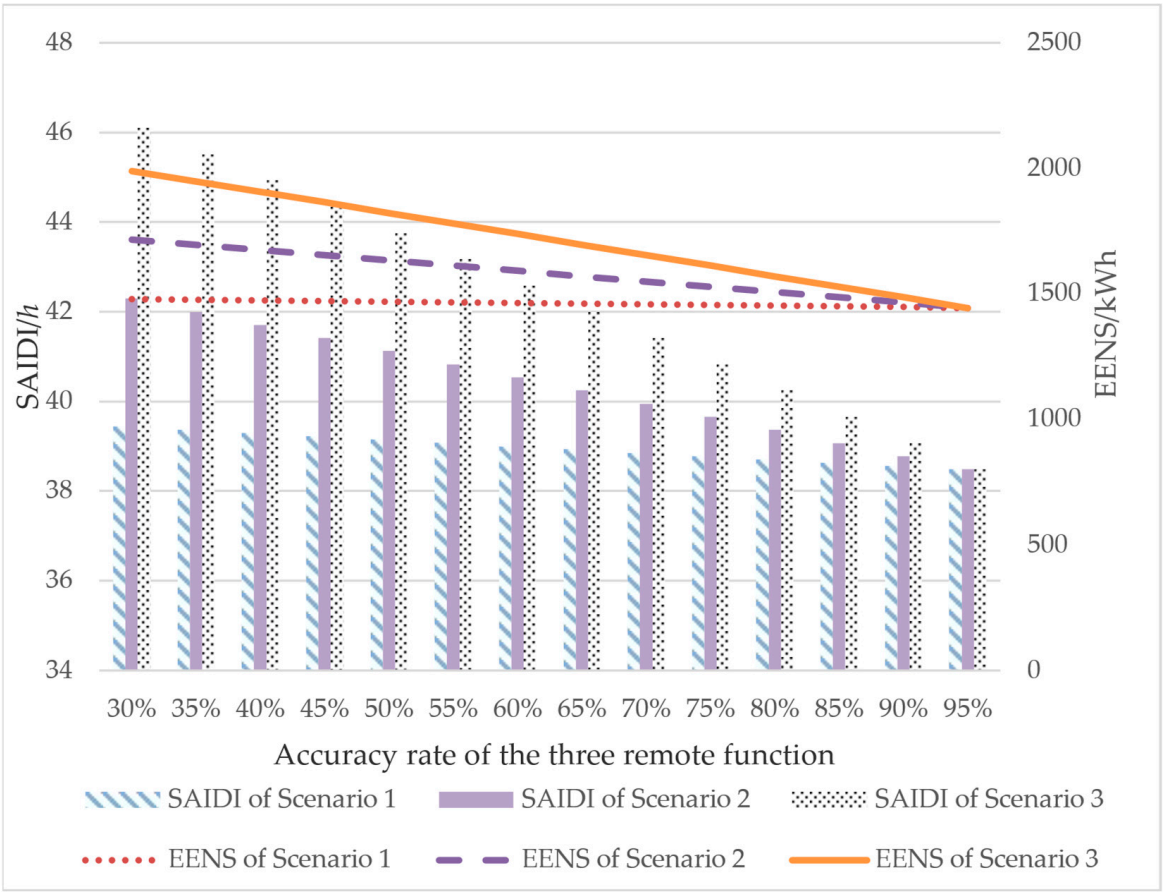

Figure 6. Influence of "3R" accuracy rate on power supply reliability and system annual energy not supplied.

It can be seen from Figure 6 that the accuracy rate of the "3R" RTU affects the SAIDI and EENS. The EENS will be reduced with the increase in the accuracy rate of the "3R" RTU. The specific growth rates are shown in Tables 8–10.

From the vertical comparison of Tables 8–10, the following conclusions can be drawn:

a. With the decrease in the accuracy rate of the remote communication function, the increase rate of the SAIDI and EENS is basically the same.
b. With the decrease in the accuracy rate of the remote measurement, the increase rate of the SAIDI and EENS is slightly reduced.
c. With the decrease in the accuracy rate of remote control, the SAIDI and EENS of the system increase greatly, which shows that the system can achieve greater economy and reliability improvements when the remote control accuracy is high.

It should be noted that, for the distribution system, even small improvements in power supply reliability are meaningful because of the high penalties imposed to utility companies for the interruption of the power supply, and the costs associated with customers claims [36]. From the horizontal comparison of Tables 8–10, the accuracy rate of the remote control, communication and measurement functions showed a significant decreasing trend regarding its impact on the reliability of the system, indicating that under the same initial investment, ensuring a high accuracy rate of the remote control function gives greater economic and reliability benefits.

6. Conclusions

This paper firstly analyzes the failure model of the distribution system, and then examines the impact of the information transmission error on the reliability indices. The proposed reliability evaluation model of power systems is established. The effectiveness

of the model and the algorithm are verified by using the IEEE 33-node system. The main conclusions drawn are as follows:

(1) Considering the large quantity and wide range of distribution RTUs with limited investment, the RTUs of a DAS cannot cover all the distribution network buses; therefore, the impact of the DA information system on the power supply reliability cannot be ignored.
(2) The rate of increase in the distribution network reliability caused by improving the accuracy rate of remote communication, remote measurement or remote control is not consistent. Therefore, in the case of limited investment, the procurement of RTU equipment is in accordance with the order of remote control, remote measurement, and remote communication.
(3) When the accuracy of the "3R" functions has to be reduced due to bad weather or unexpected reasons, the utility company should give priority to inspecting and maintaining the remote control function. It should also ensure the accuracy rate of the remote control function followed by the check and repair of remote measurement and remote communication.

The purpose of this paper is to clearly and quantitatively explain the "3R" functions in the failure handling process of the DAS, and to explain the respective impacts on the reliability of the power distribution system when the "3R" information is unreliable. The analysis framework proposed in this paper can be used to analyze various reliability indices in the case of various information system failures. It only needs to analyze the relationship between the failures and the "3R" functions, and the relationship between the "3R" functions and the reliability indicators. Therefore, the model in this paper has very good scalability. Its practical application can be adjusted according to specific situations.

Future work will take into account other factors, such as the uncertainty of the failure's repair time and the load transferability, as well as specific information system failures [37], including communication delay, communication jam, etc.

Author Contributions: Conceptualization, F.L. and N.G.; methodology, N.G.; software, F.L. and N.G.; validation, N.G. and J.X.; formal analysis, F.L.; investigation, F.L.; resources, N.G.; data curation, N.G.; writing—original draft preparation, N.G.; writing—review and editing, F.L.; visualization, F.L. and J.X.; supervision, F.L., N.G. and J.X.; project administration, J.X.; funding acquisition, J.X. All authors have read and agreed to the published version of the manuscript.

Funding: Science and Technology Projects of State Grid Corporation of China: 5400-202112571A-0-5-SF.

Data Availability Statement: Data are contained within the article.

Acknowledgments: The authors would also like to thank the anonymous reviewers for their valuable comments and suggestions to improve the quality of this paper.

Conflicts of Interest: Author Jing Xu was employed by the company State Grid Tianjin Electric Power Company. The remaining authors declare that the research was conducted in the absence of any commercial or financial relationships that could be construed as a potential conflict of interest.

References

1. Bassett, D.; Clinard, K.; Grainger, J.; Purucker, S.; Ward, D. *Tutorial Course: Distribution Automation*; Institute of Electrical and Electronics Engineers: Piscataway, NJ, USA, 1988.
2. Wang, H.; Zhong, G. Research of the self-healing technologies in the optical communication network of distribution automation. In Proceedings of the IOP Conference Series Materials Science and Engineering, Shanghai, China, 1–4 November 2018.
3. Huang, A.Q.; Baliga, J. FREEDM System: Role of power electronics and power semiconductors in developing an energy internet. In Proceedings of the 2009 21st International Symposium on Power Semiconductor Devices & IC's, Barcelona, Spain, 14–18 June 2009.
4. Liu, W.; Gong, Q.; Han, H.; Wang, Z.; Wang, L. Reliability modeling and evaluation of active cyber physical distribution system. *IEEE Trans. Power Syst.* **2018**, *33*, 7096–7108. [CrossRef]
5. Yan, D. Analysis of Safe Operation Strategy of Electrical Automation Equipment in Natural Gas Station. *Archit. Eng. Manag.* **2021**, *3*, 98–100.

6. Qinfei, W. The Design and Implementation of Intelligent Water Dispatching System. Master's Thesis, Xi'an University of Science and Technology, Xi'an, China, 2019.
7. Vellaithurai, C.; Srivastava, A.; Zonouz, S.; Berthier, R. CPIndex: Cyber-physical vulnerability assessment for power-grid infrastructures. *IEEE Trans. Smart Grid* **2015**, *6*, 566–575. [CrossRef]
8. Mello, J.C.O.; Pereira, M.V.F.; Leite Da Silva, A.M. Evaluation of reliability worth in composite systems based on pseudo-sequential Monte Carlo simulation. *IEEE Trans. Power Syst.* **1994**, *9*, 1318–1326. [CrossRef]
9. Billinton, R.; Wenyuan, L. Hybrid approach for reliability evaluation of composite generation and transmission systems using Monte-Carlo simulation and enumeration technique. *IEE Proc. C Gener. Transm. Distrib.* **1991**, *138*, 233–241. [CrossRef]
10. Billinton, R.; Wang, P. Teaching distribution system reliability evaluation using Monte Carlo simulation. *IEEE Trans. Power Syst.* **1999**, *14*, 397–403. [CrossRef]
11. Wang, P.; Billinton, R. Time sequential distribution system reliability worth analysis considering time varying load and cost models. *IEEE Trans. Power Deliv.* **1999**, *14*, 1046–1051. [CrossRef]
12. Liu, H.; Huang, J. *Reliability Evaluation for Complex Distribution System Based on the Simplified Zone Model and the Minimal Path*; IEEE Computer Society: Washington, DC, USA, 2011.
13. Xie, K.; Zhou, J.; Billinton, R. Reliability evaluation algorithm for complex medium voltage electrical distribution networks based on the shortest path. *IEE Proc. Gener. Transm. Distrib.* **2003**, *150*, 686–690. [CrossRef]
14. Billinton, R.; Wang, P. Reliability-network-equivalent approach to distribution-system-reliability evaluation. *IEE Proc. Gener. Transm. Distrib.* **1998**, *145*, 149–153. [CrossRef]
15. Li, W.; Wang, P.; Li, Z.; Liu, Y. Reliability evaluation of complex radial distribution systems considering restoration sequence and network constraints. *IEEE Trans. Power Deliv.* **2004**, *19*, 753–758. [CrossRef]
16. Cao, W.; Li, Z.; Li, Y. Optimisation Configuration of Overhead-Line Segmentation Switch of a Distribution Network Based on Global Combination Criterion. *Processes* **2022**, *10*, 1976. [CrossRef]
17. Zhang, Y.; Wang, L.; Xiang, Y.; Ten, C. Power System Reliability Evaluation with SCADA Cybersecurity Considerations. *IEEE Trans. Smart Grid* **2015**, *6*, 1707–1721. [CrossRef]
18. Hajian-Hoseinabadi, H.; Hasanianfar, M.; Golshan, M.E.H. Quantitative reliability assessment of various automated industrial substations and their impacts on distribution reliability. *IEEE Trans. Power Deliv.* **2012**, *27*, 1223–1233. [CrossRef]
19. Xin, S.; Guo, Q.; Sun, H.; Zhang, B.; Wang, J.; Chen, C. Cyber-physical modeling and cyber-contingency assessment of hierarchical control systems. *IEEE Trans. Smart Grid* **2015**, *6*, 2375–2385. [CrossRef]
20. Jiamei, Y.; Jianbing, X.; Ming, N. Impact of Communication System Interruption on Power System Wide Region Protection and Control System. *Autom. Electr. Power Syst.* **2016**, *40*, 17–25.
21. Lin, D.; Liu, Q.; Zeng, G.; Wang, Z.; Yu, T. Refined modeling and evaluation of reliability for cyber-physical system of distribution network. *Dianli Xitong Zidonghua/Autom. Electr. Power Syst.* **2021**, *45*, 92–101. [CrossRef]
22. Duckhwa, H.; Younghun, L. A study on the compound communication network over the high voltage power line for dis-tribution automation system. In Proceedings of the 2008 International Conference on Information Security and Assurance (ISA 2008), Busan, Republic of Korea, 24–26 April 2008; IEEE Computer Society: Busan, Republic of Korea, 2008; pp. 410–414.
23. Kim, J.; Tong, L. On topology attack of a smart grid: Undetectable attacks and countermeasures. *IEEE J. Sel. Areas Commun.* **2013**, *31*, 1294–1305. [CrossRef]
24. Yongfeng, L.; Liang, C.; Guoqiang, Z. Research of Distribution Automation Terminal Information Security Risk Evaluation Methods. *Autom. Instrum.* **2015**, *30*, 11–14.
25. Wang, P.; Ashok, A.; Govindarasu, M. Cyber-physical risk assessment for smart grid System Protection Scheme. In Proceedings of the 2015 IEEE Power & Energy Society General Meeting, Denver, CO, USA, 26–30 July 2015; IEEE Computer Society: Denver, CO, USA, 2015.
26. Wang, Q.; Pipattanasomporn, M.; Kuzlu, M.; Tang, Y.; Li, Y.; Rahman, S. Framework for vulnerability assessment of communication systems for electric power grids. *IET Gener. Transm. Distrib.* **2016**, *10*, 477–486. [CrossRef]
27. Meimei, Y.; Bingyao, L.; Lingzhong, H. Summary and prospect of ubiquitous power internet of things in intelligent power distribution system. *Electr. Eng.* **2020**, 88–89.
28. Yohanandhan, R.V.; Elavarasan, R.M.; Pugazhendhi, R.; Premkumar, M.; Mihet-Popa, L.; Zhao, J.; Terzija, V. A specialized review on outlook of future Cyber-Physical Power System (CPPS) testbeds for securing electric power grid. *Int. J. Electr. Power Energy Syst.* **2022**, *136*, 107720. [CrossRef]
29. Qiang, Q.; Wenze, L.; Weihao, T.; Zexiang, C.; Bowei, C.; Pei, K. An optimal deployment method of distribution edge computing terminals for software defined network. *Electr. Power Constr.* **2023**, *44*, 82–90.
30. Jianing, L.; Zhuo, S.; Ke, W.; Bowei, C.; Zexiang, C.; Zhigang, W. Elastic Configuration Method of Cloud-Edge Collaborative Resources for Distribution Internet of Things Automation Business. *Electr. Power Constr.* **2023**, *44*, 118–127.
31. Wang, Y.; Li, W.; Lu, J.; Liu, H. Evaluating multiple reliability indices of regional networks in wide area measurement system. *Electr. Power Syst. Res.* **2009**, *79*, 1353–1359. [CrossRef]
32. Falahati, B.; Fu, Y. Reliability assessment of smart grids considering indirect cyber-power interdependencies. *IEEE Trans. Smart Grid* **2014**, *5*, 1677–1685. [CrossRef]
33. Falahati, B.; Fu, Y.; Wu, L. Reliability assessment of smart grid considering direct cyber-power interdependencies. *IEEE Trans. Smart Grid* **2012**, *3*, 1515–1524. [CrossRef]

34. Wang, C.; Zhang, T.; Luo, F.; Li, P.; Yao, L. Fault incidence matrix based reliability evaluation method for complex distribution system. *IEEE Trans. Power Syst.* **2018**, *33*, 6736–6745. [CrossRef]
35. Billinton, R.; Allan, R.N. *Reliability Evaluation of Power Systems*; Plenum: New York, NY, USA, 1984.
36. Zhang, T.; Wang, C.; Luo, F.; Li, P.; Yao, L. Optimal Design of the Sectional Switch and Tie Line for the Distribution Network Based on the Fault Incidence Matrix. *IEEE Trans. Power Syst.* **2019**, *34*, 4869–4879. [CrossRef]
37. Wang, C.; Zhang, T.; Luo, F.; Li, F.; Liu, Y. Impacts of Cyber System on Microgrid Operational Reliability. *IEEE Trans. Smart Grid* **2019**, *10*, 105–115. [CrossRef]